ACS APPLIED MATERIALS & INTERFACES

Research Article

www.acsami.org

Organophosphates as Solvents for Electrolytes in Electrochemical Devices

Andrew Hess, Greg Barber, Chen Chen, Thomas E. Mallouk, and Harry R. Allcock*

Department of Chemistry, The Pennsylvania State University, University Park, Pennsylvania 16802, United States

ABSTRACT: A homologous series of fire-retardant oligoalkyleneoxyphosphates was synthesized for evaluation as liquid or gel-type electrolyte media for dye-sensitized solar cells (DSSCs) and secondary lithium batteries. Unoptimized DSSC electrolyte formulations for DSSCs achieved ionic conductivities as high as 5.71×10^{-3} S·cm^{-1} and DSSC test-cell efficiencies up to 3.6% as well as V_{oc}, J_{sc}, and ff up to 0.81 V, 8.03 mA·cm^{-2}, and 0.69, respectively. Poly(bis-(2-(2-methoxyethoxy)ethoxy)phosphazene)-based Li^+-conducting gel electrolytes plasticized with the best performing phosphate had conductivities as high as 9.9×10^{-4} S·cm^{-1} at 30 °C. All the liquids have boiling points higher than 197 °C. The results show that the viscosity, glass transition temperatures, and conductivity of the phosphates are dependent mainly on the length of the longest alkyleneoxy chain.

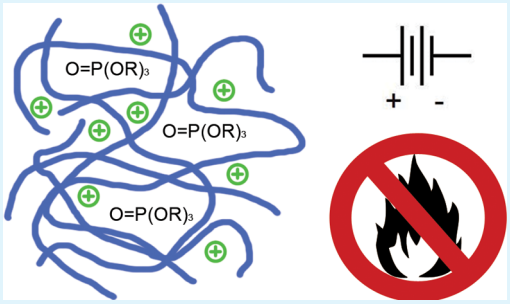

KEYWORDS: *phosphate, electrolyte, dye-sensitized solar cell, lithium batteries, fire-retardant*

1. INTRODUCTION

Dye-sensitized solar cells (DSSCs) and lithium-ion batteries are increasingly important electrochemical technologies that employ liquid electrolytes for solar power conversion and energy storage, respectively.[1,2] Although the highest performance of these devices is typically achieved with low-viscosity organic liquids, these electrolytes present manufacturing and safety challenges because of their volatility and flammability. The objective of this work has been to develop nonvolatile, fire-retardant liquids for use as electrolyte media or for use as plasticizers in gel-type electrolytes for these types of electrochemical devices.

Lithium batteries are one of the most effective ways to store electrical energy for portable devices. However, the liquid electrolytes employed in rechargeable lithium-ion batteries are a major source of operational problems.[2,3] For lithium batteries the crucial need for nonflammable or flame-retardant electrolytes has become obvious in technologies ranging from laptop computers to automobiles and aircraft. Both organophosphates and many phosphazenes are known to be fire retardants, and specific examples have been studied as polymer electrolytes.[4,5] In this work we combine these compounds to generate electrolytes that may solve these problems.

DSSCs are also a promising alternative to silicon-based solar cells due to their low raw materials cost, simple fabrication, and increasingly high-energy conversion efficiencies. Energy conversion efficiencies up to 12% have been reported when using organic solvent-based electrolytes and ruthenium complex or zinc-porphyrin sensitizers.[6−9] However, like lithium batteries, conventional DSSC electrolytes based on organic solvents suffer from problems which limit the practical use of the device such as leakage, evaporation of the solvent, and the flammability of the solvent.[10]

A large number of solid-state polymeric electrolyte formulations have been reported as proposed alternatives to the use of organic solvents in both DSSCs and lithium batteries.[11−16] However, solid polymer electrolytes suffer from lower ionic conductivities than their liquid counterparts as a result of their high viscosity. In previous research, we studied electrolyte blends based on nonvolatile and fire-retardant poly(organophosphazenes).[17,18] Electrolytes based on nonplasticized poly(bis(2-(2-methoxyethoxy)ethoxy)phosphazene) (MEEP) and lithium triflate have achieved ionic conductivities up to 3.9×10^{-5} S·cm^{-1}.[19] However, these electrolytes are limited by insufficient conductivity caused by high viscosity. Plasticized compositions based on this same polymer have ionic conductivities higher than 1.5×10^{-4} S·cm^{-1}.[4]

Tris(2-(2-methoxyethoxy)ethyl)phosphate is an effective electrolyte additive and fire retardant for lithium batteries.[18,20] Such organophosphates are valuable either as liquid electrolyte media or polymer gel-electrolyte plasticizers.[5,21] As such they show promise as flame-retardant additives or replacements for organic carbonates in lithium batteries and in DSSC electrolytes. Organophosphates would also be useful to plasticize polymers and polymer gel-electrolytes in place of more volatile organic plasticizers. Such organophosphates have high boiling points, are fire retardant, and produce highly conductive electrolytes. However, little was known about the effect of the length of the alkyleneoxy chains on either viscosity or ionic conductivity.

A homologous series of organophosphate solvents (Table 1) was prepared to probe the structure−property relationship of

Received: September 10, 2013
Accepted: December 4, 2013
Published: December 4, 2013

Table 1. Structures and Spectral Characterization of Organophosphate Electrolyte Media

Entry	Molecular Weight	Structure	^{31}P NMR (ppm, $CDCl_3$)	^{1}H NMR (ppm, $CDCl_3$)
1	140.07		2.69 (s)	3.64 (d, 9H)
2	184.13		1.77 (s)	4.13 (m, 2H), 3.73 (d, 6H), 3.56 (td, 2H), 3.35 (s, 3H)
3	228.18	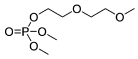	1.64 (s)	4.11 (m, 2H), 3.69 (d, 6H), 3.63 (m, 2H), 3.57 (m, 2H), 3.46 (m, 2H), 3.29 (s, 3H)
4	228.18	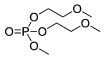	0.65 (s)	4.10 (m, 4H), 3.70 (d, 3H), 3.52 (td, 4H), 3.30 (s, 6H)
5	272.23	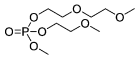	0.59 (t)	4.14 (m, 4H), 3.76 (d, 3H), 3.69 (m, 2H), 3.61 (m, 2H), 3.56 (m, 2H), 3.50 (m, 2H), 3.34 (s, 3H), 3.32 (s, 3H)
6	272.23	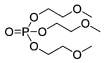	-0.45 (s)	3.98 (m, 6H), 3.39 (t, 6H), 3.17 (s, 9H)
7	316.29	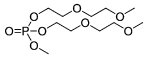	0.59 (s)	4.18 (m, 4H), 3.76 (d, 3H), 3.69 (t, 4H), 3.63 (m, 4H), 3.52 (m, 4H), 3.35 (s, 6H)
8	316.29	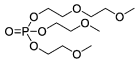	-0.40 (s)	4.17 (m, 6H), 3.70 (td, 2H), 3.63 (m, 2H), 3.58 (td, 4H), 3.52 (m, 2H), 3.36 (s, 6H), 3.35 (s, 3H)
9	360.34	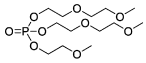	-0.52 (s)	4.18 (m, 6H), 3.70 (td, 4H), 3.64 (m, 4H), 3.58 (td, 2H), 3.52 (m, 4H), 3.37 (s, 3H), 3.36 (s, 6H)
10	404.39	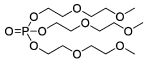	-0.60 (s)	4.07 (m, 6H), 3.58 (t, 6H), 3.51 (m, 6H), 3.40 (m, 6H), 3.24 (s, 9H)

the solvents with their physical properties and performance as electrolytes. The organophosphates were prepared by a modification of a published procedure to produce species with varying alkyleneoxy chain lengths.[20] Phosphoryl chloride was treated with alkyleneoxy alcohols in the presence of triethylamine as a proton acceptor in the presence of 4-dimethylaminopyridine as a catalyst (Scheme 1). The products

Scheme 1. General Synthesis of Organophosphate Electrolyte Media

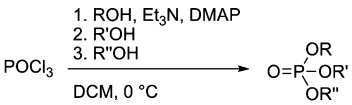

R= CH_3, $CH_2CH_2OCH_3$ (ME), or $CH_2CH_2OCH_2CH_2OCH_3$ (MEE)

were then evaluated as candidates for DSSC electrolyte media by measuring viscosity, boiling point, and conductivity and by utilization in test cells. The compound which performed best as a liquid electrolyte was further tested as a plasticizer for gel-type lithium-ion conducting electrolytes.

2. EXPERIMENTAL SECTION

Standard Schlenk techniques were employed to isolate the reactive starting materials from the atmosphere and moisture. Phosphoryl chloride (Aldrich), phosphorus pentoxide (Alfa Aesar), and 4-dimethylaminopyridine (DMAP) (TCI) were used as received. Ultrapure dichloromethane (DCM) and triethylamine were obtained from a solvent purifying and dispensing system. 2-Methoxyethanol (Aldrich), 2-(2-methoxyethoxy)ethanol (Aldrich), and methanol (EMD) were distilled over sodium metal and were stored over molecular sieves under dry argon before use.

Synthesis of 6 and 10. The following procedure is typical for compounds **6** and **10**. A solution of phosphoryl chloride (60.00 g, 0.391 mol, 1 equiv) in DCM (100 mL) was added dropwise over the course of 2 h to a solution of 2-methoxyethanol (119.11 g, 1.565 mol, 4.0 equiv), triethylamine (166.31 g, 1.643 mol, 4.2 equiv), and 4-dimethylaminopyridine (4.78 g, 0.039 mol, 0.1 equiv) in DCM (500 mL) at 0 °C with magnetic stirring. The reaction mixture was allowed to warm slowly to room temperature and was stirred for 18 h. The mixture was filtered to remove precipitated triethylamine hydrochloride, and the filtrate was washed with 5% HCl (3 × 200 mL). The combined aqueous layers were back-extracted with DCM (2 × 50 mL). The combined organic layers were dried over $MgSO_4$, and DCM was removed by rotary evaporation to yield clear faint yellow oils. The crude product was then distilled under vacuum to yield clear colorless oil (81.98 g, 77%).

Synthesis of 4, 5, and 7−9. The following procedure is typical for compounds **4**, **5**, and **7−9**. A solution of 2-methoxyethanol (59.55 g, 0.78 mol, 2.0 equiv), triethylamine (138.60 g, 1.37 mol, 3.5 equiv), and DMAP (4.78 g, 0.04 mol, 0.1 equiv) in DCM (200 mL) was added dropwise over the course of 2 h to a stirred solution of phosphoryl chloride (60.00 g, 0.39 mol, 1.0 equiv) in DCM (300 mL) held at 0 °C by an ice bath. Immediately after completion of the first dropwise addition, 2-(2-methoxyethoxy)ethanol (56.42 g, 0.47 mol, 1.2 equiv) was added in one portion, and the mixture was allowed to warm slowly to room temperature while being stirred overnight. The mixture was filtered to remove precipitated triethylamine hydrochloride, and the filtrate was reduced to 500 mL by rotary evaporation of DCM. The concentrated solution was washed with 5% HCl (3 × 200 mL) and deionized water (3 × 100 mL). The combined aqueous layers were back-extracted with DCM (2 × 50 mL). The combined organic layers were then dried over $MgSO_4$, and DCM was removed by rotary evaporation to yield clear yellow oil (104.94 g, 85%). The product was further purified by stirring over activated carbon in DCM solution, filtration, and distillation under vacuum to yield clear colorless oil (85.87 g, 69%).

Synthesis of 2 and 3. The following procedure was used for compounds **2** and **3**. A solution of 2-(2-methoxyethoxy)ethanol (51.72 g, 0.43 mol, 1.1 equiv) and triethylamine (138.59 g, 1.37 mol, 3.5 equiv) in DCM (100 mL) was added dropwise over the course of 3 h to a stirred solution of phosphoryl chloride (60.00 g, 0.39 mol, 1.0 equiv) in DCM (300 mL) held at 0 °C by an ice bath. Immediately after the completion of the first dropwise addition, methanol (26.33 g, 0.82 mol, 2.1 equiv) was added slowly via syringe, and the mixture was allowed to warm slowly to room temperature while being stirred overnight. The mixture was filtered to remove precipitated triethylamine hydrochloride, and the filtrate was reduced to 500 mL by rotary evaporation of DCM. The concentrated solution was washed with 5% HCl (3 × 200 mL) and deionized water (3 × 100 mL). The combined aqueous layers were back-extracted with DCM (2 × 50 mL). The combined organic layers were dried over $MgSO_4$ and stirred over alumina (50 g, Brockmann I, acidic) to adsorb pyrophosphates. The mixture was filtered and distilled under vacuum to yield clear colorless oil (14.21 g, 16%).

Characterization. ^{31}P NMR (145 MHz) and ^{1}H NMR (360 MHz) data were obtained using a Bruker 360 MHz spectrometer. ^{31}P NMR spectra were referenced to external 85% phosphoric acid. ^{1}H NMR spectra were referenced to external tetramethylsilane.

The viscosity of each phosphate was measured on a Low Shear Contraves LS30 rheometer using a steady shear method. All viscosity measurements were taken at 25 °C using at least two different shear rates. Boiling points were measured under a stream of argon at atmospheric pressure using the inverted bell-capillary technique and were corrected to standard pressure. Sub-boiling thermal properties were characterized using a TA Instruments DSC-Q10 heating from −150 to 50 °C at a rate of 10 °C·min^{-1}.

DSSC electrolyte samples were prepared by dissolving 3-methyl-1-propylimidazolium iodide, iodine, *n*-butyl-benzimidazole, and guanidi-

nium thiocyanate in the organophosphate solvent by stirring at room temperature. The conductivity of each electrolyte was measured by electrochemical impedance spectroscopy (EIS) using a Solartron 1260 impedance analyzer with a two-electrode custom-built cell. The temperature of the electrolyte was controlled during measurement by immersing the cell in a regulated oil bath. The system was allowed to equilibrate at each temperature for at least 30 min.

A series of gel-electrolytes were prepared by dissolving poly(bis(2-(2-methoxyethoxy)ethoxy)phosphazene) (MEEP) in **4** with a prescribed amount of lithium triflate in a sealed vial at approximately 80 °C. A sample of each electrolyte was loaded into a custom-built cell, and the conductivity was measured by the same technique as for the DSSC electrolytes, except that the temperature was controlled during measurements by using an oven.

DSSC Test Cells. Nanocrystalline titania cells were constructed on 1" × 1" fluorine-doped tin oxide (FTO, Pilkington Glass, 8 Ohm cm, 3 mm thick) by the doctor blading technique. In particular, the FTO was cleaned with acetone and IPA, and then a section of the FTO was covered with Kapton tape to ensure good electrical contact to the FTO under testing. A titania underlayer was formed on the substrates by spin coating a 0.2 M solution of titanium diisopropoxide bis(acetylacetonate) in isopropyl alcohol onto the substrates at 2400 rpm for 30 s. The substrates were then heated to 400 °C in a box oven for 20 min. After cooling to room temperature, the substrates were coated with a nanocrystalline titania paste and heated to 450 °C at 5 °C per minute in a box furnace with ambient air environment. The samples were held at 450 °C for 30 min, and the nanocrystalline films were nominally 9 μm thick. After cooling to nominally 80 °C, the samples were sensitized by being placed in a 5 mM solution of $(Bu_4N^+)_2[Ru(dcbpyH)_2(NCS)_2]^{2-}$ (N719, dcbpy = 4,4′-dicarboxy-2,2-bipyridine) in a 50:50 (v:v) mixture of acetonitrile:*tert*-butanol for 24–48 h.[22]

The electrolyte solution was a modified version of the Z946 electrolyte reported in the literature.[23] All concentrations and compounds were the same as reported in the literature except that 1-methyl-3-propylimidazolium iodide (Sigma-Aldrich) was used in place of 1,3-dimethylimidazolium iodide.

The platinum cathode was constructed by sputter coating an FTO substrate first with 20 nm of chromium and then 200 nm of platinum by DC magnetron sputtering. The cathodes were then cut to size, rinsed with acetone, isopropyl alcohol, and ethanol, and then dried under a nitrogen stream. The surface of the cathode was then coated with a 0.1 mM solution of chloroplatinic acid in isopropanol by spin coating before being heated to 350 °C at 5 °C/min in the same box furnace that was used for titania anode processing. The counter-electrodes were held at 350 °C for 15 min before cooling to ambient temperature.

The cells were constructed and tested using a stretched Parafilm spacer between the anode and cathode such that the distance between the anode and cathode was approximately 30–40 μm. The cells were held together with binder clips to minimize electrolyte loss during testing. Before the planar cells were filled with electrolyte and sealed, the anode films were scraped down to a size of either 8 mm × 10 mm or 5 mm × 5 mm with a stainless steel razor blade.

Solar testing was performed on the sealed cells under nominally AM1.5 Global 1 sun conditions. The incident radiation for device current–voltage was from a 150 W Xe lamp (Newport-Oriel, CT, USA) passing through a matched pair of AM1.0 and AM1.5 optical filters. For current–voltage measurements, the intensity was set to "1 sun" by using a calibrated silicon solar cell (Burdick Laboratories) and a short wavelength bandpass filter (<700 nm, Edmund Optics). "1 sun" was set by matching the measured current of this calibrated silicon cell covered by the short pass filter under illumination from the 150 W light source to the same cell covered with the same short pass filter under irradiance from a Class A solar simulator (Newport-Oriel, CT, USA).

3. RESULTS AND DISCUSSION

Synthesis of Organophosphate Solvents. The organophosphate solvents were synthesized by treating phosphoryl chloride with alcohols in the presence of triethylamine and 4-dimethylaminopyridine (DMAP) catalyst. Unwanted pyro- and polyphosphate formation occurred (indicated by peaks near −13.2 ppm in ^{31}P NMR spectra) in reactions when DMAP catalyst was omitted and in reactions that were stirred for extended periods of time before the addition of enough alcohol to complete chlorine substitution. Therefore, it is preferable either to add the phosphoryl chloride to an excess of alcohol or to add the next alcohol in the synthesis immediately after completing the addition of the previous alcohol. Counter-intuitively, syntheses targeting compounds **2** and **3** proceeded with fewer side reactions when uncatalyzed. However, these syntheses still resulted in some pyrophosphate formation. Fortunately, it was found that the pyrophosphates are adsorbed by activated alumina, and this characteristic was exploited to separate the desired phosphates from the side products.

Conductivity of Electrolytes. The temperature-dependent conductivity plots of the electrolytes (Chart 1) show Arrhenius

Chart 1. Arrhenius Plots of Organophosphate Electrolyte Conductivity

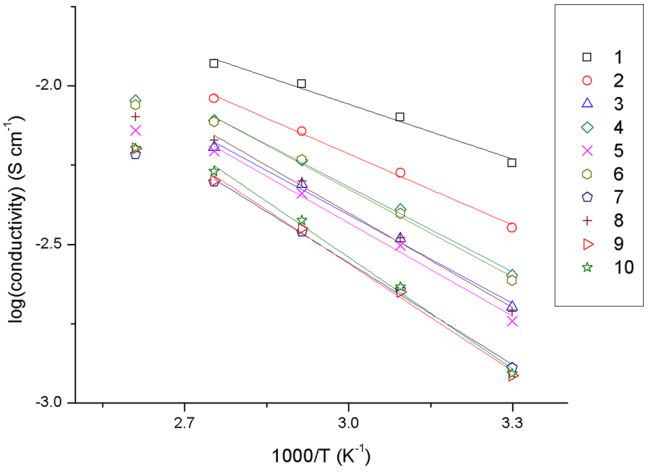

behavior. This is not surprising since all of the organophosphates were well above their T_g's during all measurements. Therefore, the conduction mechanism is based on a simple drift of the charge carriers, and the viscosity of the electrolyte plays an important role in determining the conductivity. A less viscous electrolyte should result in lower activation energy of the ion diffusion process and therefore higher conductivity (Chart 2). This is reflected in the activation energies obtained by fitting the data to the Arrhenius equation (Chart 3). It should be noted that at very high electrolyte concentrations charge transport by exchange reactions of the iodide/tri-iodide redox couple begins to dominate over ionic diffusivity.[24,25] However, the concentrations employed in this study were not high enough to observe this effect.

The electrolyte prepared from phosphate **1** gave the highest room-temperature ionic conductivity (Table 2). However, **1** is the least desirable for use in actual DSSCs or batteries because it has the lowest boiling point. Furthermore, electrolytes from phosphates **1**–**3** lost iodine at the highest temperature tested (indicated by a change in color). This indicates that the lower molecular weight phosphates are less satisfactory solvents for

Chart 2. Comparison of Viscosity and Conductivity

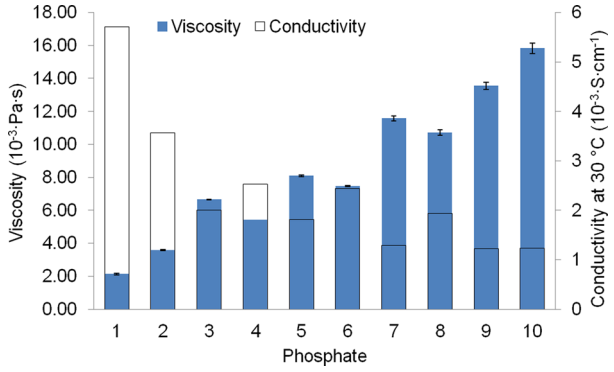

Chart 3. Activation Energy of Organophosphate Electrolytes

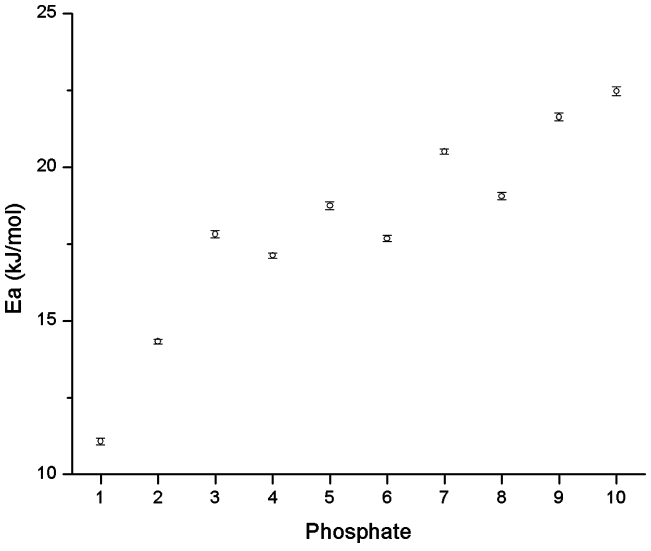

Table 2. Summary of the Properties of the Organophosphate Electrolyte Media

entry	viscosity (10^{-3}·Pa·s)	σ (S·cm^{-1}) at 30 °C	T_g (°C)	bp (°C)
1	2.14	5.71×10^{-3}	−131.20	197
2	3.58	3.57×10^{-3}	−113.55	250.4
3	6.66	2.01×10^{-3}	−102.08	265.1
4	5.43	2.53×10^{-3}	−103.45	282.2
5	8.09	1.82×10^{-3}	−96.80	277.7
6	7.47	2.44×10^{-3}	−98.11	dec.
7	11.58	1.29×10^{-3}	−91.94	dec.
8	10.72	1.94×10^{-3}	−92.62	dec.
9	13.55	1.22×10^{-3}	−90.57	dec.
10	15.83	1.24×10^{-3}	−86.99	dec.

iodine than those containing longer side chains. For this reason, the highest-temperature data points were not included when fitting the data to the Arrhenius equation.

Relationship between the Viscosity of the Organophosphates and the Organic Chain Length. The viscosity of the electrolyte has a direct effect on the conductivity and therefore on the efficiency of the cell. The viscosities of the organophosphates corresponded well with the conductivity of their respective electrolytes. When the series of electrolytes is viewed in order, a decrease in conductivity is found each time the viscosity of the organophosphate increases. The viscosity of each organophosphate is reported in Table 2. The viscosities of the phosphates decrease with decreased molar mass and increase with increased side chain length. It was initially speculated that greater asymmetry might result in a lower viscosity due to the higher entropy. However, the data show that side chain length dominates viscosity dependence. Even those phosphates with identical molar masses but different chain lengths have different viscosities. A comparison of **5** and **6** demonstrates this observation. Despite **5** having greater asymmetry, it still has a higher viscosity than **6** because it contains a longer chain.

Relationship between the Glass Transition of Organophosphates and Molecular Mobility. Differential scanning calorimetric (DSC) analysis was carried out to characterize the thermal properties of the phosphates. No distinct melting transitions were observed in the DSC traces of any of the compounds except **10**. However, each compound underwent a step-type transition from a glassy to a liquid state, reported here in Table 2. The temperature of these transitions provides another measure of the molecular mobility of the compound. This is because molecules with greater mobility have less of a tendency to form glasses and therefore have a lower T_g. In other words, the glass forming tendency of a substance is greater the lower the energy necessary to produce a given amount of disorder.[26] Therefore, it was expected that asymmetry would facilitate glass formation. The data suggest that for similarly sized compounds asymmetry certainly contributes to glass forming ability. However, the T_g is dominated by the chain length rather than by degree of symmetry. This is reflected in the fact that higher T_g's were detected for compounds with longer chains despite their having greater symmetry.

Volatility of the Organophosphates. It is important for the eventual application of these electrolytes that they have a low volatility to avoid problems caused by vapor losses and leakage. The measured boiling points of the organophosphates are reported in Table 2 as an indicator of their relative volatility. All the compounds boil at or above 197 °C, and overall, the boiling point of each compound increases with molecular weight as expected. However, the higher molecular weight compounds tend to decompose before reaching their boiling point. For this reason, boiling points at atmospheric pressure could not be reported for compounds **6**–**10**. The high boiling point of these compounds makes them good choices for electrolyte solvents where volatility is undesirable.

Cells Using the Lower Viscosity Electrolytes are More Efficient. Overall DSSC efficiencies and photovoltaic parameters of test-scale cells are reported in Table 3. Compound **1** had the highest overall cell efficiency (3.6%). However, it is also the most volatile. Species **4** and **6** appear to offer the best compromise between low volatility and cell efficiency. Test cells

Table 3. Photovoltaic Parameters of DSSC Test Cells

entry	J_{sc} (mA·cm^{-2})	V_{oc} (V)	ff	η (%)
1	6.48	0.81	0.69	3.6
2	7.35	0.76	0.61	3.4
3	7.27	0.79	0.58	3.3
4	7.38	0.75	0.56	3.1
5	7.21	0.74	0.49	2.6
6	8.03	0.75	0.51	3.1
7	6.48	0.74	0.45	2.2
8	7.67	0.75	0.50	2.9

could not be constructed with **9** or **10** due to the high viscosity of the electrolytes, which prevented complete penetration of the liquid into the porous TiO_2 electrode. The current densities and device performances were quite respectable considering that the TiO_2 films were only 9 μm thick and no scattering layers were employed.

Conductivity of Polymer-Gel Electrolytes. Since **4** has the best combination of properties in the case of a DSSC electrolyte, it was further tested as a plasticizer in gel-type electrolytes for lithium batteries. A series of gel-electrolytes were prepared based on lithium triflate dissolved in MEEP and plasticized with phosphate **4** (P4). Additional electrolytes based on poly(ethylene oxide) (PEO) for comparison were not tested since it was discovered that PEO is insoluble in **4**. The formulation of the electrolytes is detailed in Table 4, and the conductivity results are presented in Chart 4.

Table 4. Composition of Gel-Electrolyte Samples[a]

	MEEP (mol)	LiTf (mol)	P4 (mol)	P4 (mass %)	O/Li+
MEEP(0)-30	1	0.2	0	0	30
MEEPP(15.0)-30	1	0.25	0.25	15.0	30
MEEPP(31.2)-30	1	0.33	0.66	31.2	30
MEEPP(48.7)-30	1	0.5	1.5	48.7	30
MEEPP(67.5)-30	1	1	4	67.5	30
LiqP4(100)-30		1	5	100	30

[a]Sample designations are as follows: Numbers in parentheses represent the mass percentage of phosphate **4** (neglecting the mass of LiTf), while numbers after the dash represent the ratio of oxygen atoms to lithium ions in the electrolyte.

Chart 4. Arrhenius Plots of Gel-Electrolyte Conductivity

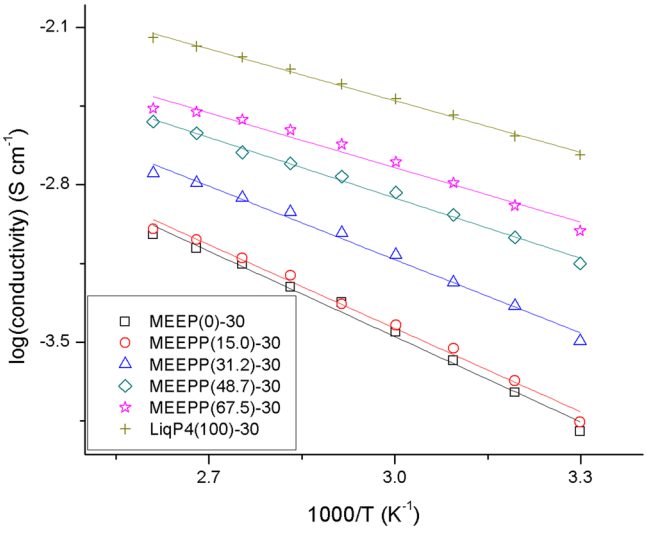

Since all testing was carried out well above the T_g of any of the components of the electrolytes the data were fitted to a linear trendline since it should exhibit purely Arrhenius-type behavior. It is clear that a larger proportion of **4** results in higher conductivity. Therefore, phosphate **4** is considered an effective plasticizer for MEEP-based lithium conducting gel-electrolytes.

4. CONCLUSIONS

The properties of the organophosphates described here, such as viscosity and conductivity, are dominated by the length of the longest chain present in the phosphate. Conductivity and cell efficiency depend on the viscosity of the solvent because mass transport is limited by solvent viscosity. Of the compounds studied, **4** has the best combination of properties and performance for use in DSSCs. The low volatility and fire-retardant properties of these organophosphates make them an attractive alternative to conventional organic solvents in DSSC and lithium batteries.

AUTHOR INFORMATION

Corresponding Author

*E-mail: hra@chem.psu.edu.

Notes

The authors declare no competing financial interest.

ACKNOWLEDGMENTS

We thank the U.S. Department of Energy for financial support (Grant DE-FG36-08GO18011).

REFERENCES

(1) Hagfeldt, A.; Boschloo, G.; Sun, L.; Kloo, L.; Pettersson, H. *Chem. Rev.* **2010**, *110*, 6595−6663.
(2) Tarascon, J. M.; Armand, M. *Nature* **2001**, *414*, 359−367.
(3) Wang, Q.; Ping, P.; Zhao, X.; Chu, G.; Sun, J.; Chen, C. *J. Power Sources* **2012**, *208*, 210−224.
(4) Fei, S.; Allcock, H. R. *J. Power Sources* **2010**, *195*, 2082−2088.
(5) Xu, K.; Ding, M. S.; Zhang, S.; Allen, J. L.; Jow, T. R. *J. Electrochem. Soc.* **2002**, *149*, 622−626.
(6) Nazeeruddin, M. K.; De Angelis, F.; Fantacci, S.; Selloni, A.; Viscardi, G.; Liska, P.; Ito, S.; Takeru, B.; Grätzel, M. *J. Am. Chem. Soc.* **2005**, *127*, 16835−47.
(7) O'Regan, B.; Gratzel, M. *Nature* **1991**, *353*, 737−740.
(8) Yella, A.; Lee, H.-W.; Tsao, H. N.; Yi, C.; Chandiran, A. K.; Nazeeruddin, M. K.; Diau, E. W.-G.; Yeh, C.-Y.; Zakeeruddin, S. M.; Grätzel, M. *Science* **2011**, *334*, 629−634.
(9) Robertson, N. *Angew. Chem., Int. Ed. Engl.* **2006**, *45*, 2338−2345.
(10) Wu, J.; Lan, Z.; Hao, S.; Li, P.; Lin, J.; Huang, M.; Fang, L.; Huang, Y. *Pure Appl. Chem.* **2008**, *80*, 2241−2258.
(11) Wu, J.; Lan, Z.; Hao, S.; Li, P.; Lin, J. *Pure Appl. Chem.* **2008**, *80*, 2241−2258.
(12) Nest, J.; Le Gandini, A.; Cheradame, H. *Br. Polym. J.* **1988**, *20*, 253−268.
(13) Petrov, P.; Berlinova, I.; Tsvetanov, C. B.; Rosselli, S.; Schmid, A.; Zilaei, A. B.; Miteva, T.; Durr, M.; Yasuda, A.; Nelles, G. *Macromol. Mater. Eng.* **2008**, *293*, 598−604.
(14) Karan, N. K.; Pradhan, D. K.; Thomas, R.; Natesan, B.; Katiyar, R. S. *Solid State Ionics* **2008**, *179*, 689−696.
(15) Xiang, W.; Zhou, S.; Yin, X.; Xiao, X.; Lin, Y. *Polym. Adv. Technol.* **2009**, *20*, 519−523.
(16) Suzuki, K.; Yamaguchi, M.; Hotta, S.; Tanabe, N.; Yanagida, S. *J. Photochem. Photobiol. A: Chem.* **2004**, *164*, 81−85.
(17) Lee, S. A.; Jackson, A. S.; Hess, A.; Fei, S.; Pursel, S. M.; Basham, J.; Grimes, C. A.; Horn, M. W.; Allcock, H. R.; Mallouk, T. E. *J. Phys. Chem. C* **2010**, *114*, 15234−15242.
(18) Morford, R. V; Welna, D. T.; Iii, C. E. K.; Hofmann, M. A.; Allcock, H. R. *Solid State Ionics* **2006**, *177*, 721−726.
(19) Allcock, H. R.; Kuharcik, S. E.; Reed, C. S.; Napierala, M. E. *Macromolecules* **1996**, *29*, 3384−3389.
(20) Morford, R. V; Kellam, E. C.; Hofmann, M. A.; Baldwin, R.; Allcock, H. R. *Solid State Ionics* **2000**, *133*, 171−177.
(21) Wang, X.; Yasukawa, E.; Kasuya, S. *J. Electrochem. Soc.* **2001**, *148*, 1058−1065.

(22) Ito, S.; Murakami, T. N.; Comte, P.; Liska, P.; Grätzel, C.; Nazeeruddin, M. K.; Grätzel, M. *Thin Solid Films* **2008**, *516*, 4613−4619.
(23) Wang, M.; Chen, P.; Humphry-baker, R.; Zakeeruddin, S. M.; Grätzel, M. *ChemPhysChem* **2009**, *10*, 290−299.
(24) Kawano, R.; Matsui, H.; Matsuyama, C.; Sato, A.; Bin, A.; Susan, H.; Tanabe, N.; Watanabe, M. *J. Photochem. Photobiol. A: Chem.* **2004**, *164*, 87−92.
(25) Bai, Y. U.; Cao, Y.; Zhang, J.; Wang, M.; Li, R.; Wang, P.; Zakeeruddin, S. M.; Grätzel, M. *Nat. Mater.* **2008**, *7*, 626−630.
(26) Turnbull, D.; Cohen, M. H. *J. Chem. Phys.* **1961**, *34*, 120−125.